Oral Oncology 98 (2019) 85–91

Contents lists available at ScienceDirect

Oral Oncology

journal homepage: www.elsevier.com/locate/oraloncology

A multidimensional nomogram combining overall stage, dose volume histogram parameters and radiomics to predict progression-free survival in patients with locoregionally advanced nasopharyngeal carcinoma

Kaixuan Yang[a,1], Jiangfang Tian[a,1], Bin Zhang[b,1], Mei Li[a,1], Wenji Xie[a], Yating Zou[c], Qiaoyue Tan[a], Lihui Liu[a], Jinbing Zhu[a], Arthur Shou[d], Guangjun Li[a,*]

[a] Department of Radiation Oncology, Cancer Center and State Key Laboratory of Biotherapy, West China Hospital, Sichuan University, Chengdu, Sichuan 610041, China
[b] Department of Radiology, The First Affiliated Hospital of Jinan University, Guangzhou, Guangdong, China
[c] Department of Biostatistics, Gillings School of Public Health, University of North Carolina-Chapel Hill, Chapel Hill, NC 27599, United States
[d] School of Basic Medical Sciences and Forensic Medicine, Sichuan University, Chengdu, Sichuan 610041, China

ARTICLE INFO

Keywords:
Locoregionally advanced nasopharyngeal carcinoma
Radiomics
Intensity modulated radiotherapy
Dose volume histogram parameters
Lymph node
Nomogram

ABSTRACT

Objectives: To develop a multidimensional nomogram for predicting the progression-free survival (PFS) in patients with locoregionally advanced nasopharyngeal carcinoma (NPC) (stage III-IVa).

Materials and methods: A total of 224 patients with locoregionally advanced NPC (training cohort, n = 149; validation cohort, n = 75) were retrospectively included. We extracted 260 radiomic features from the primary tumor and lymph nodes on the axial contrast-enhanced T1 weighted and T2 weighted MRI. Radiomic signatures of the gross tumor volume (RSnx) and lymph node (RSnd), Dose Volume Histogram (DVH) signature reflecting planning score (PS), and clinical characteristics were included as potential predictors of PFS. The least absolute shrinkage and selection operator (LASSO) regression were applied for feature selection and data dimension reduction. A nomogram was developed by incorporating the selected predictors. The C-index and calibration curve were used to assess discrimination and calibration power of the nomogram, respectively.

Results: RSnd, PS, and tumor-node-metastasis (TNM) stage were the independent predictors for PFS (all $p < 0.05$). The nomogram integrating the three factors achieved a C-index of 0.811 (95% CI: 0.74–0.882) in the validation cohort for predicting PFS, which outperformed than that of the TNM stage alone (C-index, 0.613, 95% CI: 0.532–0.694). Subgroup analysis showed Epstein–Barr virus (EBV) DNA status improved the predictive accuracy of the nomogram (C-index, 0.86, 95% CI: 0.787–0.933).

Conclusions: The multidimensional nomogram incorporating RSnd, PS, and TNM stage showed high performance for predicting PFS in patients with locoregionally advanced NPC.

Introduction

Nasopharyngeal carcinoma (NPC) is a highly prevalent malignant tumor in South China. More than 70% of NPC are categorized as locoregionally advanced disease [1]. Despite advances in radical chemoradiotherapy, distant metastasis and locoregional recurrence are still the primary causes of treatment failure, especially the former [2]. The treatment outcomes of locoregionally advanced NPC is unsatisfactory, with 5-year overall survival of 67–77%. Only 72.9% of cases have a 2-year PFS after the initiation of treatment [3]. Hence, it is essential to improve the outcome of those patients.

High-throughput extraction through data-characterization algorithms from medical images is an emerging and attractive method for objective and quantitative evaluation of tumor heterogeneity [4]. radiomic analysis from multiparametric MRI has been successfully performed to predict individual PFS in advanced NPC [5,6]. However, These studies only focused on radiomic feature derived from primary nasopharynx gross tumor volume (GTVnx). A recent research demonstrated primary and lymph nodes (LNs)-metastatic tumors possess different biological characteristics [7]. The sentinel lymph nodes are prone to metastasis. Therefore, precision medicine needs to consider personal metastatic regional lymph node (GTVnd) information added to the primary tumor based radiomics.

Radiotherapy is the cornerstone treatment of NPC. Numerous

* Corresponding author at: No. 37, GuoXue Alley, Chengdu, Sichuan, China.
E-mail address: gjnick829@sina.com (G. Li).
[1] Contributed equally to this work.

https://doi.org/10.1016/j.oraloncology.2019.09.022
Received 13 June 2019; Received in revised form 24 August 2019; Accepted 21 September 2019
Available online 27 September 2019
1368-8375/

studies have elucidated how dosimetric parameters affect the prognosis of NPC [8]. However, they did not consider all significant dose-volume histogram parameters (DVHs), nor anatomical variations of region of interest (ROI) and its relationship with dosimetric consequences [9].

The least absolute shrinkage and selection operator (LASSO) regression is a robust statistical method based on cross-validation, which can fix the multicollinearity problem in high dimensional data. Through this penalized analysis, meaningful factors can be preserved to generate a more accurate predictor panel [10]. Therefore, LASSO is recommended for normal tissue complication probability prognosticators selection [11]. We used LASSO to select the useful predictors from the mass data of primary tumor, regional lymph nodes, and DVH parameters based radiomic features.

We aimed to develop and validate a nomogram considering the potential of clinical data, GTVnx/GTVnd based radiomic signature, and multiparametric based therapeutic DVHs signature by LASSO. Our model provides an individualized assessment of 3-year and 5-year PFS probability in patients with locoregionally advanced NPC.

Methods and materials

Patients

This retrospective study was approved by the institutional review board of our institution. Informed consent from patients was exempted due to the retrospective nature of this study. A dataset of 310 patients with newly diagnosed locoregionally advanced NPC (stage III-IVa) were included from January 2010 to February 2013. The inclusion criteria were as follows: (1) histologically-confirmed advanced NPC (restage according to AJCC/UICC 8th edition[14]); (2) patients underwent pretreatment MRI examinations; (3) patients were treated with curative radiotherapy; (4) patients without previous radiotherapy, surgery, and/or chemotherapy; and (5) patients with available clinical data. The exclusion criteria were: (1) with motion artifacts on MRI images; and (2) radiotherapy planning failed to be restored. Supplementary Fig. S1 shows the patient flowchart. Finally, a total of 224 patients were included for further analysis. The patients were randomly divided into the training cohort (n = 149) and validation cohort (n = 75) using random number table at a ratio of approximately 2:1. Fig. 1 presents the radiomic workflow, including MRI images acquisition and segmentation, feature extraction and selection, and modeling.

Patients' characteristics were collected consisting of age, sex, body mass index (BMI), family history of cancer, cigarette smoking, alcohol consumption, pretreatment Epstein–Barr virus (EBV) DNA, hemoglobin (Hb), platelet count (PLT), neutrophil count, lymphocyte count, neutrophil-lymphocyte-ratio (NLR), lactate dehydrogenase (LDH), T stage, N stage, TNM stage, GTVnx, GTVnd, WHO histological type, radiotherapy duration days (RDD), radiotherapy modality, image-guided radiotherapy (IGRT), chemotherapy regimens, the use of cetuximab, and clinical endpoints. The methodology for collection and analysis of EBV-DVA was provided in the Supplementary Methods.

MRI acquisition and segmentation

All patients underwent 1.5 T MRI scans (Trio, Siemens, Germany). For the axial contrast- enhanced T1-weighted (CET1W) spin-echo images, TR/TE: 1970/2.3 ms, FOV = 24 × 24 cm, NEX = 2.0, slice thickness = 5 mm, interslice gap = 1.5 mm; for the axial T2-weighted (T2W) spin-echo images, TR/TE: 7300/89 ms, FOV = 24 × 24 cm, NEX = 2.0, slice thickness = 5 mm, interslice gap = 1.5 mm. CET1WI and T2WI were obtained from the Picture Archiving and Communication System (PACS) for each patient. Without any processing or standardization, we imported the Digital Imaging and Communications in Medicine (DICOM) formatted images into a commercial software system, Raystation (Raysearch Laboratories, Sweden). All targeted image segmentations of the GTVnx/GTVnd were firstly manually performed by a radiation oncologist who had four years of experience in NPC radiotherapy, and then validated by a senior radiation oncologist who has 10 years of experience. The ROI covers the entire tumor on each slice. GTVnx and GTVnd were defined and then delineated as visible primary tumor and all the lymph nodes [12], respectively, on each slice of the axial CET1WI and the T2WI images.

Feature selection and radiomic signature building

LIFEx (Version 4.0) was an open-source, multi-platform, and easy-to-use freeware that could be used to acquire multimodality radiomic features of medical imaging [13]. A total of 260 quantitative radiomic features (65 per sequence) were calculated from GTVnx and GTVnd for each patient. We extracted two types of features, including the first-order features (indices from shape, indices from histogram, and conventional indices) and texture features (grey level co-occurrence matrix [GLCM], neighborhood grey-level different matrix [NGLDM], grey-level run length matrix [GLRLM], and grey-level zone length matrix [GLZLM]). A detailed feature description is available in the Texture User Guide of LIFEx (www.lifexsoft.org) or Supplementary Texture User Guide.

We used the radiotherapy planning data archived in the mosaiq system (Elekta Medical Systems, Sun-nyvale, CA, USA). After transferring the data to Raystation, we extracted the planning parameters through our in-house script run by raystation system (Supplementary Text). A total of 12 DVH parameters were achieved for each patient, including PGTVnx_D2, PGTVnx_D50, PGTVnx_D95, PGTVnx_D98, PGTVnx_CI, PGTVnx_HI, PGTVnd_D2, PGTVnd_D50, PGTVnd_D95, PGTVnd_D98, PGTVnd_CI, and PGTVnd_HI.

The LASSO was a regression method that involves penalizing the absolute size of the regression coefficients. We used LASSO to select the PFS status associated features among the above-mentioned high dimensional data. Adjusted by λ, the LASSO scheme could shrink each coefficient towards zero and tailor the coefficients to zero for insignificant parameters. We then chose the λ for which the cross-validation error is the smallest. The parameters with non-zero coefficients were thus selected by LASSO to build the regression model. The RSnx (radiomic signature of GTVnx), RSnd (radiomic signature of GTVnd), PS (planning score) of DVH were calculated for each patient as a linear combination of the values of the selected features that were weighted by their respective coefficients, respectively.

Construction and validation of the nomogram

After features selected by LASSO, we firstly conducted a univariate Cox proportional hazards regression analysis to determine the PFS-prediction ability of RSnx, RSnd, PS and clinical data with the training cohort. For those factors with $p < 0.05$, we then tested them in backward step-wise selection by using the likelihood ratio test with Akaike's information criterion as the stopping rule [14]. Finally, we incorporated the independent risk factors of PFS into nomogram.

In the nomogram, a risk score for each patient was calculated based on the linear predictor function "predict" in R software, which was used for prediction from the results of Cox model fitting functions. The predictive performance of the nomogram was evaluated by discrimination and calibration ability. A concordance index (C-index) was used to evaluate the discrimination power of nomogram, which was calculated by 1000 bootstrap resamples in 3-year and 5-year PFS. In addition, the discriminative ability of nomogram was assessed via time-dependent receiver operating characteristic curve (tdROC) analysis. We compared the area under time-dependent ROC curve (tdAUC) of nomogram and TNM stage in the prediction of 3-year and 5-year PFS using "survivalROC" package in R software. We used the calibration curve to compare the actual PFS against the prediction probability of nomogram.

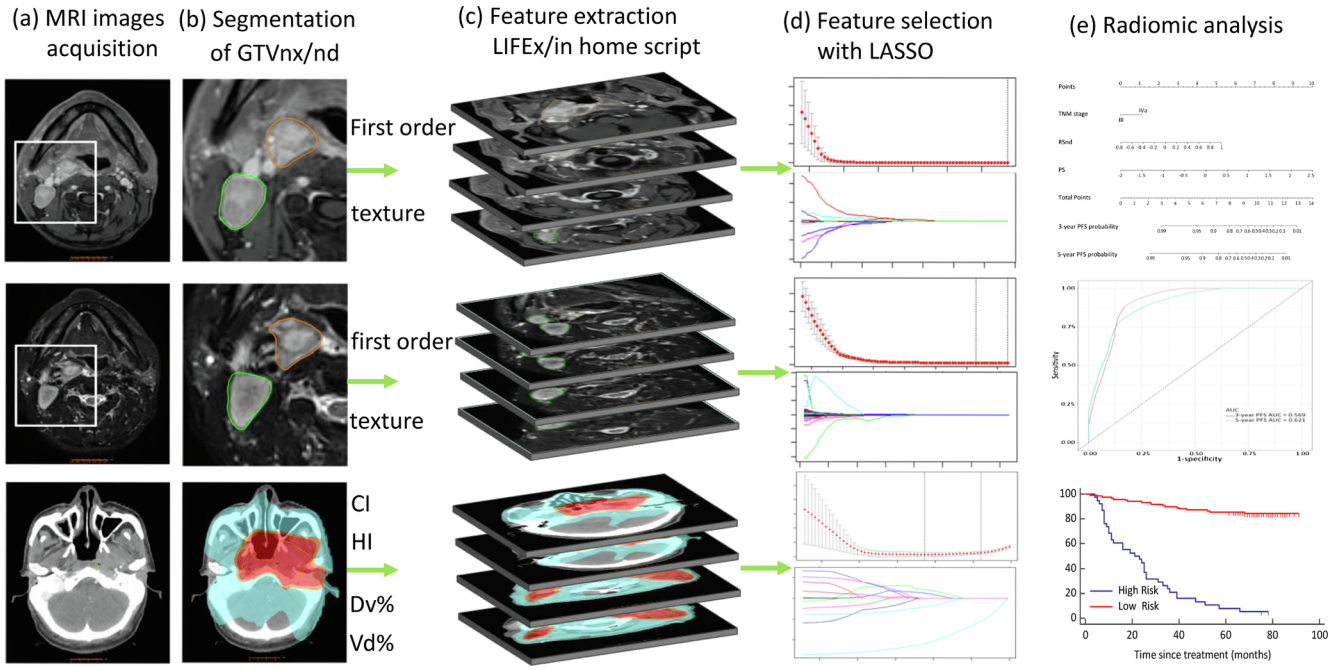

Fig. 1. Radiomic signature building workflow, including (a) MRI images acquisition; (b) and segmentation of GTVnx/nd; (c) feature extraction using LIFEx/in house script; (d) feature selection using LASSO with 10-fold cross validation; and (e) radiomic modeling. Abbreviation: CI = conformal index; HI = homogeneity index; Vd % = the volume exposed in d Gy; Dv% = the minimal dose delivered into v% of the volume; LASSO = The least absolute shrinkage and selection operator; GTVnx = nasopharynx gross tumor volume; GTVnd = lymph node gross tumor volume.

Risk classification of patients

The optimal cutoff value of the risk score was determined by the X-tile software (version 3.6.1; Yale University, New Haven, CT, USA) in the training cohort. We then classified all patients into low- or high- risk groups according to the optimal cutoff value that produced the largest χ^2 value in the Mantel–Cox test [15]. The log-rank test was performed to compare the survival curves of the different risk groups in the training and validation cohorts.

Statistical analysis

All statistical analyses were conducted using SPSS (version 22.0), MedCalc (version 15.6), and R software (version 3.5.2). The following R packages were implemented: LASSO logistic regression was completed by the "glment" package. "Rms" package was for nomogram and calibration curves. The comparison of C-index was performed by using "Hmisc" package. The Kaplan–Meier survival analyses were presented by MedCalc. A $P < 0.05$ was considered as statistically significant.

Results

Patient characteristics and signature construction

Patient characteristics of the training and validation cohorts are summarized in Table 1. No significant differences were observed between the two cohorts besides the radiotherapy duration time ($p = 0.006$). Median PFS was 39 months (ranges, 2–68 months) and median follow-up was 68 months (ranges, 2–100 months).

Of the 260 MRI-derived radiomic features, 130 features were extracted from GTVnx and the remaining 130 were from GTVnd. Among them, three GTVnx features (GLCM_Energy, GLCM_Corre, and CONV_std) were used to build the RSnx, and another three GTVnd features (Shape_Compacity, GLCM_Energy, and Kurtosis) were used to build the RSnd. The equations of RSnx and RSnd were as follows: RSnx = −0.033 * GLCM_Energy − 0.021 * GLCM_Corre − 0.07 * CONV_std; RSnd = 0.247 * Shape_Compacity − 0.069 * GLCM_Energy + 0.004 * Kurtosis. According to the Radiation Therapy Oncology Group (RTOG) Protocol 0534 and International Commission on Radiation Units & Measurements (ICRU) report 83, 12 DVH metrics were extracted using our in-house script. Out of the 12 DVH metrics, three metrics (PGTVnx_D95, PGTVnx_CI, and PGTVnd_CI) associated with PFS in the training cohort were selected to construct the PS signature (Fig. 1). The equation of PS was: PS = 0.004 * PGTVnx_D95 − 0.727 * PGTVnx_CI − 0.037 * PGTVnd_CI.

Nomogram development and validation

In the univariate Cox analysis, T stage, N stage, TNM stage, volume of GTVnd, RSnx, RSnd, and PS were associated with PFS in Table 2 (for all, $p < 0.05$). Subsequent multivariate Cox analysis showed TNM stage (HR, 2.275, 95% CI: 1.172–4.418), RSnd (HR, 11.153, 95% CI: 4.149–19.99), and PS (HR, 5.445, 95% CI: 3.461–8.565) were three independent risk factors for PFS. According to coefficients of risk factors in the multivariate analyses, a nomogram was developed visually to quantify the probability of 3-year and 5-year PFS (Fig. 2A). The calibration curves of the nomogram showed good calibration in predicting 3- and 5-year PFS (Fig. 2B–C).

The nomogram achieved excellent performance in predicting PFS, with C-index of 0.843 (95% CI: 0.798–0.888) in the training and 0.811 (95% CI: 0.74–0.882) in the validation cohort. The predictive ability of nomogram was better than that of the TNM staging system in the training cohort (C-index, 0.592, 95% CI: 0.529–0.655) and validation cohort (C-index, 0.613, 95% CI: 0.532–0.694). The ROC of the TNM stage and nomogram for predicting 3-year and 5-year PFS are presented in Fig. 3A–B. The combined nomogram (3-year PFS: AUC, 0.879, 95% CI: 0.851–0.936; 5-year PFS: AUC, 0.897, 95% CI: 0.867–0.961) outperformed than the TNM staging system (3-year PFS: AUC, 0.603, 95% CI: 0.524–0.663; 5-year PFS: AUC, 0.618, 95% CI: 0.535–0.689) in the training cohort. Similarly, when tested in the validation cohort, the performance of nomogram (3-year PFS: AUC, 0.802, 95% CI: 0.786–0.872; 5-year PFS: AUC, 0.847, 95% CI: 0.811–0.964) was also

Table 1
Characteristics of all patients (n = 224).

	Training cohort (n = 149)	Validation cohort (n = 75)	p value
Age (years)	45.7 ± 10.5	49.7 ± 10.4	0.339
Sex			0.628
Male	106 (71)	51 (68)	
Female	43 (29)	24 (32)	
BMI (kg/m^2)	22 (20.2–24.8)	22.1 (20.2–25.8)	0.948
Family history of cancer			0.515
No	120 (81)	64 (85)	
Yes	29 (19)	11 (15)	
Cigarette smoking			0.886
No	77 (52)	38 (51)	
Yes	72 (48)	37 (49)	
Alcohol consumption			0.793
No	109 (73)	54 (72)	
Yes	40 (27)	21 (28)	
Hb (g/L)	140.8 ± 13.3	140.7 ± 15.4	0.342
PLT ($\times 10^9$/L)	209.6 ± 58.8	201.5 ± 66.9	0.239
Neutrophil count ($\times 10^9$/L)	4.2 (3.3–4.9)	4.2 (3.2–5.0)	0.668
Lymphocyte count ($\times 10^9$/L)	1.5 (1.2–1.9)	1.6 (1.3–2.0)	0.743
NLR	2.7 (2.0–3.4)	2.4 (1.9–3.3)	0.778
LDH (IU/L)	174 (156.5–199)	182 (152.3–216)	0.667
AJCC/UICC 8th TNM stage			0.742
III	57 (38)	27 (36)	
Iva	92 (62)	48 (64)	
T stage			0.16
T2	3 (2)	0	
T3	87 (58)	37 (49)	
T4	59 (40)	38 (51)	
N stage			0.769
N0	2 (1)	2 (3)	
N1	14 (9)	9 (12)	
N2	89 (60)	45 (60)	
N3	44 (30)	19 (25)	
GTVnx (cc)	55.8 (35.9–79.3)	50.6 (39.4–73)	0.782
GTVnd (cc)	9.1 (4.9–17.9)	11.28 (6.7–24.3)	0.946
WHO histological type			0.411
Keratinizing SqCC	0	1 (1)	
Non-Keratinizing, Differentiated	121 (81)	63 (84)	
Non-Keratinizing, Undifferentiated	25 (17)	9 (12)	
unspecified	3 (2)	2 (3)	
RDD	47 (44–49.5)	49 (47–52)	0.006
Radiotherapy modality			0.121
IMRT	134 (90)	62 (83)	
VMAT	15 (10)	13 (17)	
IGRT			0.229
No	118 (79)	54 (72)	
Yes	31 (21)	21 (28)	
Chemotherapy			
IC	20/129	7/68	0.375
CC	43/106	31/44	0.085
AC	86/63	45/30	0.744
Cetuximab			0.597
No	123 (83)	64 (85)	
Yes	26 (17)	11 (15)	
Clinical endpoints			0.795
none	98 (66)	47 (63)	
recurrence	11 (7)	8 (11)	
distant metastasis	20 (13)	10 (13)	
recurrence and distant metastasis	3 (2)	0	
death	17 (11)	10 (13)	

Note: Data are shown as means (standard deviation), medians (interquartile ranges) or numbers (%). BMI = body mass index; Hb = Hemoglobin; PLT = Platelets; NLR = Neutrophil Lymphocyte Ratio; LDH = Lactate dehydrogenase; GTVnx = nasopharynx gross tumor volume; GTVnd = lymph node gross tumor volume; cc = cubic centimeter; RDD = Radiotherapy duration days; IMRT = Intensity-Modulated Radiation Therapy; VMAT = volumetric modulated arc radiotherapy; IGRT = image-guided radiotherapy.

higher than the TNM staging system (3-year PFS: AUC, 0.585, 95% CI: 0.521–0.68; 5-year PFS: AUC, 0.637, 95% CI: 0.543–0.747).

The pre-treatment EBV-DNA data were available in 74 (49.7%), 58 (77.3%) patients in the training and validation cohorts, respectively. Considering the pretreatment EBV-DNA has been showed to be a useful prognostic biomarker in NPC [16]. We thus conducted subgroup analysis to explore its additional value to this present model. The results showed better performance of nomogram (C-index, 0.916, 95% CI: 0.874–0.958) after adding EBV-DNA, which was confirmed in the validation cohort, with C-index of 0.86 (95% CI: 0.787–0.933). Supplementary Fig. S2 shows the AUC of pre-treatment EBV-DNA was 0.610, and the optimal cutoff value was 4010 copies/mL, with a sensitivity of 0.643 and specificity of 0.667.

Identification of high- and low-risk groups of patients

Based on the optimal cutoff point identified by the X-tile plots, patients with a linear prediction score ≥1 were classified into the high-risk group (n = 36) and those with linear prediction score < 1 were classified as low-risk group (n = 113). Notably, K-M survival curves showed the PFS of high-risk group was much lower than the low-risk group ($p < 0.001$) in the training cohort (Fig. 4A) and validation cohort (Fig. 4B).

Discussion

In this study, we established and validated a nomogram to individually predict PFS in patients with locoregionally advanced NPC. The results showed that TNM stage, RSnd, and PS are independent prognosticators of PFS. The nomogram significantly outperformed the 8th AJCC TNM staging system for predicting 3-year and 5-year PFS. Its performance could be improved by adding the pre-treatment EBV-DNA. Using the risk scores derived from the model, we successfully classified patients into low- and high- risk groups.

The association between radiation dose and clinical outcome haven't been paid any attention until Mijnheer et al. [17] and Wittkämper et al. [18], by performing dosage analyses in various institutions, proved this relationship. In the study, the dosimetric parameters that most strongly associated with PFS, were GTVnx D95, GTVnx CI, and GTVnd CI. As one of RTOG 0534 recommended constraints, the dose to 95% of the volume (D95) was the most popular prescription point among academic institutions [19]. It has been commonly used as an intensity modulated radiotherapy (IMRT) plan criteria [20]. The conformal index is a helpful apparatus to represent the degree of conformality. A higher conformation means a superior therapeutic ratio [21]. After LASSO, we included three DVHs mentioned above in the PS to quantify radiotherapy benefits reasonably.

Note that, RSnd instead of RSnx was the significant risk factor of PFS in this study. The finding differed from previous studies [5,6], in which GTVnx-based MRI radiomics was a meaningful prognostic biomarker of PFS in advanced NPC. It may due to that GTVnd-based radiomics were not investigated in previous studies. A recent research demonstrated that the volumetric reduction ratios of GTVnd after induction chemotherapy, but not GTVnx, were significantly associated with 2-year PFS in advanced NPC [22]. Among the three features of GTVnd based radiomic signature, "SHAPE_Compacity" indicates how compact is the region of interest. We hypothesized this shape distribution reflects what a smallest transverse diameter of nd is, a crucial indicator of whether a lymph node is suspicious or not [12]. "Kurtosis" can assess tumor heterogeneity in forms of data histograms via computing the voxel intensities, and the gray level co-occurrence matrix "GLCM_Energy" could reveal tumor spatial complexity."Kurtosis" and "GLCM_Energy" may provide the information about central necrosis or tumor metastasis dependent factor such as yes-associated protein [7].

Pre-treatment plasma EBV DNA status improved the predictive

Table 2
Identification of risk factors of PFS by univariate and multivariate Cox models.

	Univariate cox regression		Multivariate cox regression	
	HR (95% CI)	P	HR (95% CI)	P
Age (years)	1.001(0.975–1.026)	0.967	–	–
Sex (female vs. male)	1.148(0.635–2.073)	0.648	–	–
BMI (kg/m^2)	1.002(0.907–1.107)	0.967	–	–
Family history of cancer (no vs. yes)	1.133(0.552–2.329)	0.733	–	–
Cigarette smoking (no vs. yes)	1.146(0.662–1.985)	0.627	–	–
Alcohol consumption (no vs. yes)	0.907(0.483–1.703)	0.762	–	–
Hb (g/L)	0.988(0.969–1.007)	0.211	–	–
PLT ($\times 10^9$/L)	1.002(0.998–1.006)	0.381	–	–
Neutrophil count ($\times 10^9$/L)	1.103(0.908–1.339)	0.324	–	–
Lymphocyte count ($\times 10^9$/L)	0.881(0.528–1.47)	0.628	–	–
NLR	1.129(0.916–1.391)	0.254	–	–
LDH (IU/L)	0.999(0.994–1.005)	0.73	–	–
TNM stage (III vs. IVa)	2.329(1.218–4.451)	**0.011**	2.275(1.172–4.418)	**0.015**
T stage	1.784(1.046–3.044)	**0.034**	2.331(0.764–4.173)	0.343
N stage	1.822(1.147–2.896)	**0.011**	1.85(0.925–3.587)	0.741
GTVnx (cc)	1.001(0.994–1.010)	0.667	–	–
GTVnd (cc)	1.006(1.001–1.011)	**0.023**	2.947(0.806–3.928)	0.111
WHO type	1.218(0.711–2.088)	0.473	–	–
RDD	0.983(0.948–1.019)	0.354	–	–
IMRT vs. VMAT	1.076(0.427–2.708)	0.877	–	–
IGRT (without vs. with)	0.66(0.31–1.403)	0.28	–	–
Chemotherapy (without vs. with)				
IC	0.942(0.424–2.092)	0.884	–	–
CC	1.062(0.574–1.964)	0.849	–	–
AC	1.131(0.652–1.964)	0.661	–	–
Cetuximab (without vs. with)	0.43(0.171–1.083)	0.073	–	–
RSnd	7.037(2.812–17.61)	< **0.001**	11.153(4.149–19.99)	< **0.001**
RSnx	2702(30–245709)	< **0.001**	9.066(0.05–1642.67)	0.25
PS	4.121(2.881–5.895)	< **0.001**	5.445(3.461–8.565)	< **0.001**

Note: HR = hazard ratio; CI = confidence intervals; BMI = body mass index; Hb = Hemoglobin; PLT = Platelets; NLR = Neutrophil Lymphocyte Ratio; LDH = Lactate dehydrogenase; GTVnx = nasopharynx gross tumor volume; GTVnd = lymph node gross tumor volume; cc = cubic centimeter; RDD = Radiotherapy duration days; IMRT = Intensity-Modulated Radiation Therapy; VMAT = volumetric modulated arc radiotherapy; IGRT = image-guided radiotherapy; RSnd = radiomic signature of GTVnd; RSnx = radiomics signature of GTVnx; PS = Dose Volume Histogram signature reflecting planning score.

accuracy of the model in a subgroup analysis, which was consistent with previous study [10] High EBV DNA level is associated with local recurrence and distant metastasis because it reveals tumor biological behavior and burden [10,23]. However, the optimal cutoff of plasma EBV DNA level for risk classification remains undetermined. In this study, the cutoff value was 4010 copies/mL, with a sensitivity of 0.643 and specificity of 0.667. Effort have been done to improve harmonised assays by a National Cancer Institute EBV testing harmonisation workshop for nasopharyngeal carcinoma [24]. It is promising to incorporate pre-treatment plasma EBV DNA in future revisions of the TNM staging system [16].

There are three major strengths of this study. First, it has been proved that genomically- distinct populations are one of the reasons why clinical heterogeneity of radiotherapy therapeutic benefit [25]. It is well-known that radiomics is hypothesized to illustrate the histological heterogeneity of solid tumor [26]. Although more than 90% stage III–IVa NPC patients are with positive lymph nodes, GTVnd was ignored in previous studies [5,6]. We integrated not only GTVnx- but also GTVnd-based MRI radiomics to logically describe the tumor biological characteristics. Second, most of state-of-the-art Dosimetric studies used Pearson's correlation analysis to decrease the degree of multicollinearity. It will abandon other parameters which have a smaller Spearman's correlation coefficients [27]. To avoid discarding potentially useful three dimensional doses messages [28], we constructed PS signature to gather significant DVHs reasonably via LASSO with 10-fold cross-validation. Last but not the least, RSnx was no longer an independent prognosticator of PFS when DVHs were taken into consideration. It may be that the locoregional control has enhanced substantially as the medical profession has evolved into an intensity modulated radiotherapy era [29]. Therefore, we suggested that lymph nodes should be the major target volumes that deserve more attention in the future.

Some limitations of the present study are being addressed. First, although the RSnd was validated in different admission time cohorts, due to the lack of stability in interpretation [30], repetition and comparison of different studies are difficult. In this study, the feature extraction tool LIFEx was dedicated to gather multicenter data of usefulness and limitations of radiomics in the real world setting [13]. Furthermore, the shape features and GLCM which were used as GTVnd-radiomic signature were proved to be stable features [31,32]. Second, the normalization of radiotherapy plans has been demonstrated to affect dosimetric end points [33]. However, the value of DVHs signature needed be validated in prospective studies. Third, although our sample size was in consistence with the suggestion from Chalkidou et al. [34], the CI range of RSnx was too wide in the univariate analysis. This might indicate that the sample size is relatively small, or the GTVnx of NPC has a wide range of genetic variation [25].

In summary, we established and validated a novel nomogram involving DVHs signature, GTVnd based radiomic signature, and TNM staging system that could effectively predict the PFS in patients with advanced NPC. This model will benefit those patients with worse PFS. In future, we should be more concerned about positive lymph nodes to improve the outcome in patients with advanced NPC.

Role of the funding source

This study is funded by the National Natural Science Foundation of China (Grant No. 81472807).

Declaration of Competing Interest

The authors declare that they have no known competing financial interests or personal relationships that could have appeared to influence the work reported in this paper.

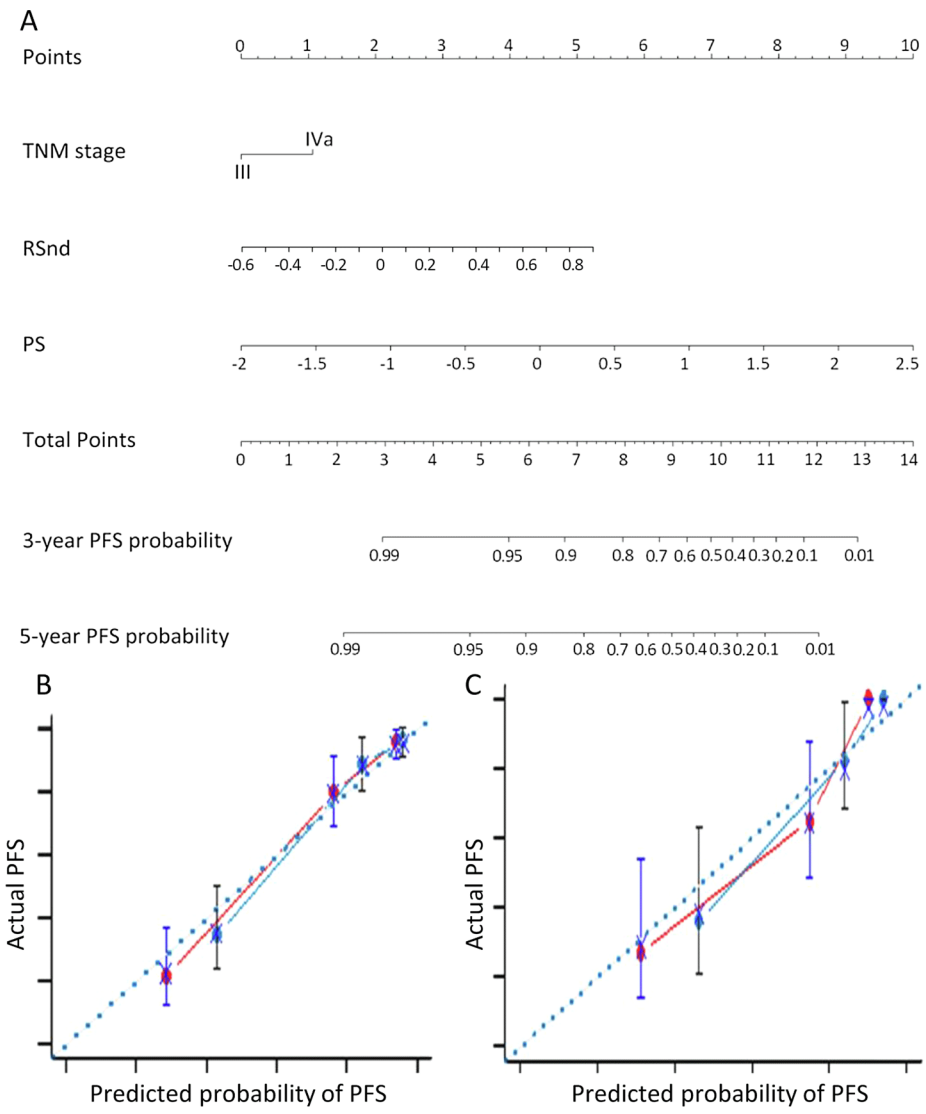

Fig. 2. Nomogram for predicting 3- and 5-year PFS (A). For each patient, the value of three variables (TNM stage, RSnd, and PS) are represented as points by projecting them onto the upper-most line (point scale). Summing the three variables and projecting the total points value downward onto the bottom-most line can determine the probability of 3-year and 5-year PFS. Calibration curves of the nomogram in the training (B) and validation cohort (C). X-axis indicates the predicted probabilities of PFS while y-axis shows the actual PFS. Abbreviation: TNM = tumor-node-metastasis; PS = planning score; RSnd = Radiomic signatures of regional lymph node.

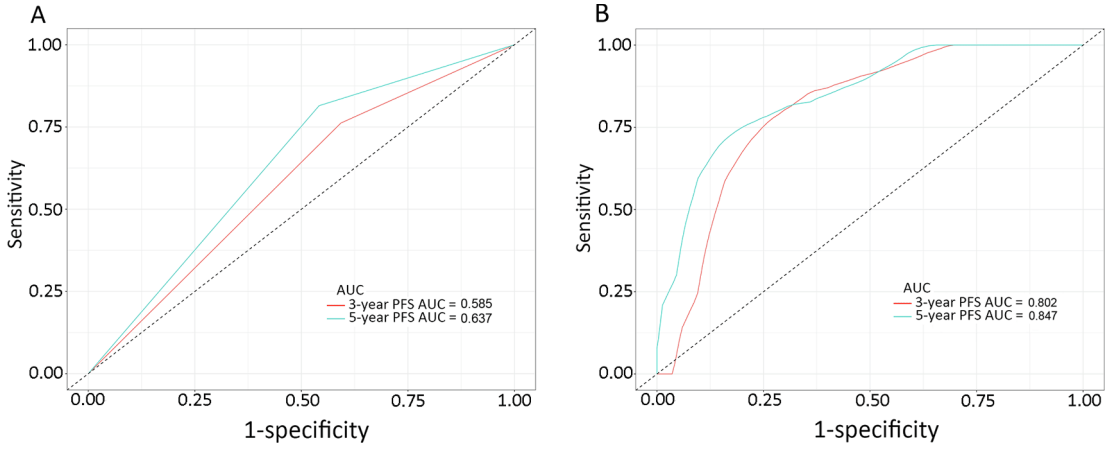

Fig. 3. The performance of the nomogram for predicting 3- and 5- year PFS. Area under the time-dependent receiver operating characteristic (tdROC) curve (AUC) of TNM stage (A) and nomogram (B) in the validation cohort.

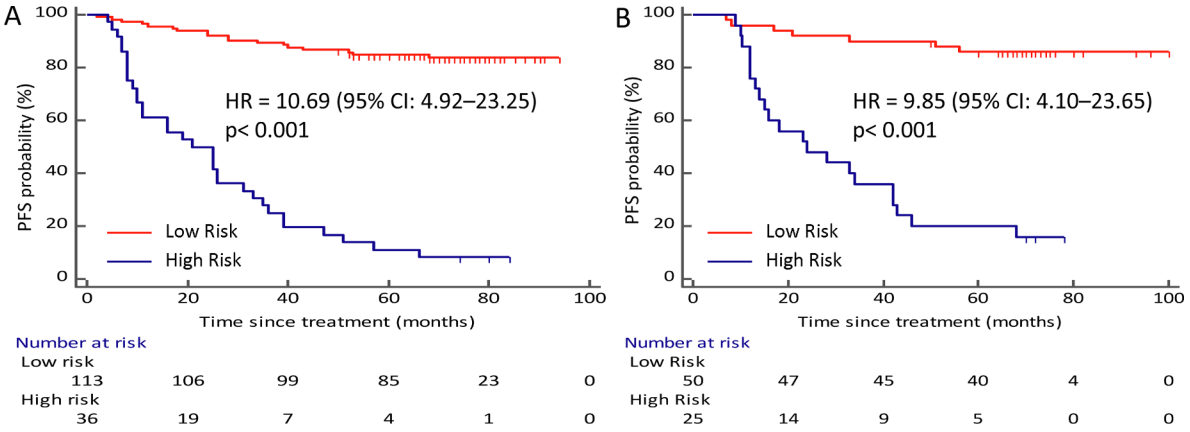

Fig. 4. Kaplan–Meier survival analyses were performed to estimate PFS of high-risk and low-risk in the training (A) and validation cohort (B). Abbreviation: HR = hazard ratio; CI = confidence intervals.

Acknowledgments

We gratefully acknowledged Ms. Yunqi Zhong for her valuable suggestions and discussions.

Informed consent

Informed consent was not necessary because this job was a retrospective study.

Appendix A. Supplementary material

Supplementary data to this article can be found online at https://doi.org/10.1016/j.oraloncology.2019.09.022.

References

[1] Pan JJ, Ng WT, Zong JF, et al. Prognostic nomogram for refining the prognostication of the proposed 8th edition of the AJCC/UICC staging system for nasopharyngeal cancer in the era of intensity-modulated radiotherapy. Cancer-Am Cancer Soc 2016(122):3307–15.
[2] Sun X, Su S, Chen C, et al. Long-term outcomes of intensity-modulated radiotherapy for 868 patients with nasopharyngeal carcinoma: an analysis of survival and treatment toxicities. Radiother Oncol 2014;110:398–403.
[3] Lee N, Harris J, Garden AS, et al. Intensity-modulated radiation therapy with or without chemotherapy for nasopharyngeal carcinoma: radiation therapy oncology group phase II trial 0225. J Clin Oncol 2009;27:3684–90.
[4] Lambin P, Rios-Velazquez E, Leijenaar R, et al. Radiomics: extracting more information from medical images using advanced feature analysis. Eur J Cancer 2012;48:441–6.
[5] Zhang B, Tian J, Dong D, et al. Radiomics features of multiparametric MRI as novel prognostic factors in advanced nasopharyngeal carcinoma. Clin Cancer Res 2017;23:4259–69.
[6] Mao J, Fang J, Duan X, et al. Predictive value of pretreatment MRI texture analysis in patients with primary nasopharyngeal carcinoma. Eur Radiol 2019.
[7] Lee CK, Jeong SH, Jang C, et al. Tumor metastasis to lymph nodes requires YAP-dependent metabolic adaptation. Science 2019;363:644–9.
[8] Ng WT, Lee MC, Chang AT, et al. The impact of dosimetric inadequacy on treatment outcome of nasopharyngeal carcinoma with IMRT. Oral Oncol 2014;50:506–12.
[9] Marks LB, Yorke ED, Jackson A, et al. Use of normal tissue complication probability models in the clinic. Int J Radiat Oncol Biol Phys 2010;76:S10–9.
[10] Tang XR, Li YQ, Liang SB, et al. Development and validation of a gene expression-based signature to predict distant metastasis in locoregionally advanced nasopharyngeal carcinoma: a retrospective, multicentre, cohort study. Lancet Oncol 2018;19:382–93.
[11] Xu C, van der Schaaf A, Schilstra C, Langendijk JA, Van T Veld AA. Impact of statistical learning methods on the predictive power of multivariate normal tissue complication probability models. Int J Radiation Oncol*Biol*Phys 2012;82:e677–84.
[12] Biau J, Lapeyre M, Troussier I, et al. Selection of lymph node target volumes for definitive head and neck radiation therapy: a 2019 Update. Radiother Oncol 2019;134:1–9.
[13] Nioche C, Orlhac F, Boughdad S, et al. LIFEx: a freeware for radiomic feature calculation in multimodality imaging to accelerate advances in the characterization of tumor heterogeneity. Cancer Res 2018;78:4786–9.
[14] Sauerbrei W, Boulesteix AL, Binder H. Stability investigations of multivariable regression models derived from low- and high-dimensional data. J Biopharm Stat 2011;21:1206–31.
[15] Camp RL, Dolled-Filhart M, Rimm DL. X-tile: a new bio-informatics tool for biomarker assessment and outcome-based cut-point optimization. Clin Cancer Res 2004;10:7252–9.
[16] Xu C, Chen YP, Liu X, et al. Establishing and applying nomograms based on the 8th edition of the UICC/AJCC staging system to select patients with nasopharyngeal carcinoma who benefit from induction chemotherapy plus concurrent chemoradiotherapy. Oral Oncol 2017;69:99–107.
[17] Mijnheer BJ, Battermann JJ, Wambersie A. What degree of accuracy is required and can be achieved in photon and neutron therapy? Radiother Oncol 1987;8:237–52.
[18] Wittkamper FW, Mijnheer BJ, van Kleffens HJ. Dose intercomparison at the radiotherapy centers in The Netherlands. 2. Accuracy of locally applied computer planning systems for external photon beams. Radiother Oncol 1988;11:405–14.
[19] Das IJ, Andersen A, Chen ZJ, et al. State of dose prescription and compliance to international standard (ICRU-83) in intensity modulated radiation therapy among academic institutions. Pract Radiat Oncol 2017;7:e145–55.
[20] Forde E, Kneebone A, Bromley R, Guo L, Hunt P, Eade T. Volumetric-modulated arc therapy in postprostatectomy radiotherapy patients: a planning comparison study. Med Dosim 2013;38:262–7.
[21] Van'T RA, Mak AC, Moerland MA, Elders LH, van der Zee W. A conformation number to quantify the degree of conformality in brachytherapy and external beam irradiation: application to the prostate. Int J Radiat Oncol Biol Phys 1997;37:731–6.
[22] Xiang Z, Liu F, Yan R, et al. The prognostic value of volumetric reduction of the target lesions after induction chemotherapy in locoregionally advanced nasopharyngeal carcinoma. Head Neck 2019.
[23] Xu M, Yao Y, Chen H, et al. Genome sequencing analysis identifies Epstein-Barr virus subtypes associated with high risk of nasopharyngeal carcinoma. Nat Genet 2019;51:1131–6.
[24] Kim KY, Le QT, Yom SS, et al. Current state of PCR-based epstein-barr virus DNA testing for nasopharyngeal cancer. J Natl Cancer Inst 2017;109.
[25] Scott Jacob G, Berglund Anders, Schell Michael J, et al. A genome-based model for adjusting radiotherapy dose (GARD): a retrospective, cohort-based study. Lancet Oncol 2017;18:202–11.
[26] Scalco E, Rizzo G. Texture analysis of medical images for radiotherapy applications. Br J Radiol 2017;90:20160642.
[27] Tang X, Li Y, Tian X, et al. Predicting severe acute radiation pneumonitis in patients with non-small cell lung cancer receiving postoperative radiotherapy: Development and internal validation of a nomogram based on the clinical and dose-volume histogram parameters. Radiother Oncol 2019;132:197–203.
[28] Giraud P, Giraud P, Gasnier A, et al. Radiomics and machine learning for radiotherapy in head and neck cancers. Front Oncol 2019;9:174.
[29] Lai SZ, Li WF, Chen L, et al. How does intensity-modulated radiotherapy versus conventional two-dimensional radiotherapy influence the treatment results in nasopharyngeal carcinoma patients? Int J Radiat Oncol Biol Phys 2011;80:661–8.
[30] Lubner MG, Smith AD, Sandrasegaran K, Sahani DV, Pickhardt PJ. CT texture analysis: definitions, applications, biologic correlates, and challenges. Radiographics 2017;37:1483–503.
[31] Fiset S, Welch ML, Weiss J, et al. Repeatability and reproducibility of MRI-based radiomic features in cervical cancer. Radiother Oncol 2019;135:107–14.
[32] Leijenaar RT, Carvalho S, Velazquez ER, et al. Stability of FDG-PET Radiomics features: an integrated analysis of test-retest and inter-observer variability. Acta Oncol 2013;52:1391–7.
[33] Stritch MA, Forde E, Leech M. The impact of intensity-modulated radiation therapy plan normalization in the postprostatectomy setting-does it matter? Med Dosim 2017;42:368–74.
[34] Chalkidou A, O'Doherty MJ, Marsden PK. False discovery rates in PET and CT studies with texture features: a systematic review. PLoS ONE 2015;10:e124165.